Vol. 04, Iss. 3 (2026) 343-354, DOI: 10.61552/JME.2026.03.004

Journal of Materials and Engineering

www.jme.aspur.rs

Research article

Silica Induced Tribological Degradation in an Industrial Pelletizer Bearing: A Multiscale Failure Analysis

Willian Aperador[a,*], Angel Díaz[a], David Sanabria[a], Daniel Vargas[a], Jorge Aponte[a]

[a] *Department of Engineering, Universidad Militar Nueva Granada, Bogotá, 110111, Colombia.*

Keywords:

Failure analysis
Rolling bearing
Silica contamination
Tribological degradation
Abrasive wear
Tribocorrosion
Predictive maintenance

* Corresponding author:

Willian Aperador
E-mail:
william.aperador@unimilitar.edu.co

Received: 9 May 2026
Revised: 17 June 2026
Accepted: 22 July 2026

ABSTRACT

Premature bearing failure is a major cause of unplanned downtime in industrial equipment operating under severe service conditions, where the interaction between wear, lubrication, and contamination accelerates material degradation. This study presents a multiscale failure analysis of an NU240 cylindrical roller bearing from the main shaft of an industrial pelletizer to identify the root cause of failure and reconstruct the degradation mechanism. Visual inspection, fractographic examination, optical microscopy, X-ray diffraction, and Fourier transform infrared spectroscopy were applied to the bearing, lubricant, and solid deposits recovered from the system. The damaged components exhibited abrasive wear, adhesive wear, cavitation, and corrosion products distributed over the raceways and rolling elements. Structural characterization identified magnetite and goethite as the predominant corrosion products, while spectroscopic analysis confirmed silica contamination in the lubricant and solid residues. The results indicate that silica particles promoted lubricant film breakdown, increased friction, and accelerated the generation of metallic wear debris, leading to a transition from abrasion-dominated wear to combined abrasion, adhesion, and tribocorrosion. A failure mechanism is proposed in which external silica contamination acts as the primary trigger of progressive tribological degradation. The proposed methodology provides a reliable approach for diagnosing bearing failures and supporting predictive maintenance strategies in lubricated industrial systems.

1. INTRODUCTION

Premature bearing failures are among the leading causes of unplanned shutdowns in rotating machinery operating under severe service conditions [1]. Rolling bearings are critical mechanical components because they support combined loads while enabling efficient power transmission with minimal friction losses [2]. Their performance directly affects the operational reliability of equipment employed in mining, agro-industrial, energy, and manufacturing sectors, where unexpected failures may result in substantial maintenance costs, production losses, and reduced equipment availability [3]. In industrial applications, inadequate lubrication and lubricant contamination are consistently recognized as the principal factors responsible for premature bearing degradation [2, 4].

From a tribological perspective, bearing service life is governed by the interaction between material properties, contact stresses, lubricant film stability, and contaminant particles entrapped within the rolling contacts. During operation, repeated rolling and sliding contacts promote the initiation and propagation of several degradation mechanisms, including abrasive wear, adhesive wear, surface fatigue, cavitation, and tribocorrosion. The evolution of these mechanisms depends primarily on the ability of the lubricant film to maintain effective surface separation and prevent direct metal-to-metal contact, thereby minimizing friction and wear particle generation [2, 5].

Among the different contaminants affecting lubricated systems, silica and quartz particles are particularly detrimental because of their high hardness and angular morphology. Once introduced into the lubricant, these particles behave as abrasive third bodies, producing micro-cutting, localized plastic deformation, and progressive material removal from raceways and rolling elements. As surface damage accumulates, lubricant film stability deteriorates, promoting adhesive wear, oxidation, and the formation of corrosion products. Recent experimental investigations have demonstrated that particle size, concentration, and hardness significantly influence wear progression, vibration response, and bearing lifetime under lubricated operating conditions [6, 7]. Moreover, field inspections have shown that particle contamination generates surface indentations that alter lubrication conditions and accelerate rolling contact fatigue [8].

Despite significant advances in laboratory tribology, most published investigations have focused on isolated variables such as contaminant size, particle concentration, friction coefficient, or vibration response under controlled experimental conditions. Consequently, relatively few studies have integrated morphological, chemical, and crystallographic evidence to reconstruct the complete degradation sequence of industrial bearings operating under real service conditions. This limitation restricts the understanding of the relationship between lubricant contamination, wear evolution, corrosion development, and the final functional collapse of rolling bearings [5, 6].

Failure analysis supported by complementary characterization techniques provides an effective methodology for identifying the root cause of bearing degradation. The integration of visual inspection, fractographic examination, optical microscopy, Fourier transform infrared spectroscopy, and X-ray diffraction enables the correlation of morphological, chemical, and structural evidence with degradation mechanisms defined in ISO 15243:2017 [9] and described in the SKF Bearing Damage Atlas [10]. This multiscale approach provides a more comprehensive understanding of tribological degradation than conventional laboratory tests because it reconstructs the complete sequence of damage under actual industrial operating conditions.

The objective of this work is to determine the failure mechanism of an NU240 cylindrical roller bearing installed on the main shaft of an industrial pelletizer through a multiscale characterization of the bearing components, lubricant, and degradation products generated during service. Whereas previous investigations of SiO_2-contaminated lubricated systems, such as those of Ikhsan et al. [6] and Ta et al. [7], have relied on controlled laboratory conditions to evaluate individual wear mechanisms separately, this work addresses a real in-service failure and proposes an integrated methodology capable of reconstructing the complete degradation sequence, from silica contamination to functional blockage of the bearing, directly from field evidence. The results demonstrate that external silica particles initiate lubricant film breakdown, promote the transition from abrasion-dominated wear to combined abrasion, adhesion, and tribocorrosion, and ultimately lead to functional blockage of the bearing. The proposed methodology contributes to predictive maintenance by providing practical criteria for contamination control, failure diagnosis, and reliability improvement in lubricated industrial rotating machinery.

2. MATERIALS AND METHODS

2.1 Component Analyzed

The investigated component was an NU240 cylindrical roller bearing installed on the intermediate shaft of an industrial Amandus Kahl pelletizer used for pelletized feed production. The bearing operated under continuous industrial service conditions, rotating at approximately 450 rpm under moderate-to-high radial loading typical of this type of equipment. The exact magnitude of the applied radial load could not be retrieved from the available maintenance records; based on the equipment specifications, it is estimated to fall within the moderate-to-high range typical of main-shaft bearings of this size. Under normal operating conditions, the lubrication oil temperature was maintained at approximately 65 °C, ensuring adequate lubricant viscosity and hydrodynamic film formation between the rolling elements and raceways. The pelletizer operated in a feed-production environment characterised by a high concentration of airborne mineral dust, particularly silica containing particles, representing a potential source of external contamination of the lubrication system.

The bearing was lubricated using an ISO VG 460 mineral oil supplied through the machine lubrication circuit. Although routine lubrication practices were performed in accordance with the maintenance programme, the lubrication circuit did not incorporate a high efficiency dedicated filtration system capable of continuously removing fine mineral particles from the circulating oil. Consequently, contaminant particles entering the system could remain suspended in the lubricant and recirculate through the bearing contacts, increasing the likelihood of abrasive wear under prolonged service conditions.

The bearing was removed twelve days after abnormal operating conditions were detected, including increased operating temperature, higher rotational resistance, and progressive loss of transmission efficiency. During the final stage of operation, the lubricant temperature increased to approximately 85 °C, indicating deterioration of the lubrication regime and increased frictional losses within the bearing assembly. Although continuous vibration monitoring was not available for the investigated equipment, routine maintenance inspections reported progressive mechanical deterioration associated with increasing rotational resistance and abnormal thermal behaviour.

Prior to failure, the lubrication system exhibited a continuous reduction in lubricant level, abnormal temperature increases, and evidence of contamination detected during routine maintenance inspections. The original lubricant was replaced with an ISO VG 460 oil; however, approximately five additional gallons were required during operation to restore the service level. Routine lubricant analyses detected wear metals and silicon particles within the manufacturer's recommended limits, although symptoms associated with progressive mechanical degradation persisted. This discrepancy between routine oil monitoring and the actual bearing deterioration constitutes one of the practical findings of this investigation, suggesting that conventional oil analyses alone may not always provide sufficient sensitivity to detect the early stages of contamination-induced failure.

The exact cumulative operating hours of the bearing before failure could not be established from the available maintenance records because this investigation was conducted retrospectively after removal of the failed component. Nevertheless, under normal operating conditions, bearings of this type are generally expected to provide several years of continuous service when appropriate lubrication and contamination control are maintained. The premature deterioration observed in the present case therefore indicates the presence of an abnormal degradation process rather than the natural exhaustion of the bearing service life.

To verify the consistency of the contamination pattern observed in the radial bearing, an axial bearing (89456M), removed from the same transmission system on 12 May 2017, was also examined. In addition, lubricant samples and solid deposits recovered from the failed bearing were collected for physicochemical characterisation and reconstruction of the failure mechanism.

2.2 Failure analysis methodology

The failure analysis was carried out through an integrated multiscale methodology combining macroscopic inspection, morphological characterization, and physicochemical analyses. The experimental procedure consisted of visual inspection and photographic documentation of the damaged bearing, controlled disassembly of the bearing assembly, optical stereomicroscopy of the damaged surfaces, chemical characterization of the lubricant by Fourier transform infrared spectroscopy (FTIR), phase identification of corrosion products and contaminants by X-ray diffraction (XRD), and correlation of the experimental evidence to reconstruct the progressive degradation mechanism. This methodology enabled the integration of morphological, chemical, and crystallographic information to identify the sequence of degradation events responsible for functional blockage of the bearing.

2.3 Visual inspection and optical characterization

The failed bearing was initially subjected to visual inspection to identify macroscopic deformation, corrosion products, surface deposits, restricted roller movement, and other evidence associated with the failure process. The bearing was subsequently disassembled by controlled cutting while preserving the integrity of the raceways, cylindrical rollers, and bronze cage. Surface contaminants and corrosion products were carefully removed following the procedure described in ASTM G1-03(2017)e1, Standard Practice for Preparing, Cleaning, and Evaluating Corrosion Test Specimens [11], using mechanical and chemical cleaning methods selected to remove corrosion products without altering the original damage morphology of the base metal.

The bearing components were examined by optical stereomicroscopy at different magnifications to identify abrasive wear, adhesive wear, cavitation, plastic deformation, material transfer, and material removal. Representative micrographs of the raceways, cylindrical rollers, and bronze cage were acquired to correlate the observed damage with the physicochemical characterization performed by FTIR and XRD.

2.4 Lubricant characterization by Fourier transform infrared spectroscopy

Lubricant samples recovered from the failed transmission system were analysed using a Nicolet iS5 Fourier transform infrared (FTIR) spectrometer (Thermo Fisher Scientific Inc., Madison, WI, USA) operating in attenuated total reflectance (ATR) mode with a zinc selenide (ZnSe) crystal. Infrared spectra were acquired over the spectral range of 4000–400 cm^{-1} with a spectral resolution of 4 cm^{-1} using 32 accumulated scans for each measurement. The acquired spectra were processed using OMNIC™ software (Thermo Fisher Scientific Inc.). Compound identification was performed using the OMNIC Spectral Library through the software's Search Library function, complemented by comparison with published reference spectra and a commercial silicon dioxide (SiO_2) reference standard (Dulling Agent HK 125). Silica contamination was confirmed by matching the characteristic Si–O–Si vibrational bands, including the asymmetric stretching band at approximately 1000–1100 cm^{-1}, the symmetric stretching band near 800 cm^{-1} and the bending vibration around 460 cm^{-1}, with those of the reference material. The spectra were further examined to identify absorption bands associated with lubricant oxidation and degradation products.

2.5 Structural characterization by X-ray diffraction

The crystalline phases present on the bearing surfaces and in the solid deposits recovered from the lubricant were identified by X-ray diffraction (XRD) using an Empyrean diffractometer (Malvern Panalytical B.V., Almelo, The Netherlands) operating in θ–2θ geometry with Cu Kα radiation (λ = 1.5406 Å). Diffraction patterns were collected over the 20–120° (2θ) range using a step size of 0.02°, a counting time of 2 s per step, and operating conditions of 40 kV and 30 mA. Phase identification was performed using X'Pert HighScore software (Malvern Panalytical B.V., Almelo, The Netherlands) in conjunction with the ICDD PDF-4+ crystallographic database. Semi-quantitative phase analysis was carried out by Rietveld refinement using the refinement module implemented in X'Pert HighScore. The refinement involved iterative fitting of the calculated diffraction pattern to the experimental data by adjusting structural and profile parameters until convergence was achieved. The resulting refined phase fractions were used to estimate the relative abundance of the identified crystalline phases and to determine the corrosion products and mineral contaminants associated with the tribological degradation of the bearing.

2.6 Failure mechanism reconstruction

The experimental evidence obtained from visual inspection, optical stereomicroscopy, Fourier transform infrared spectroscopy, and X-ray diffraction was integrated to reconstruct the progressive degradation sequence responsible for bearing failure. The correlation between surface morphology, lubricant chemistry, and crystallographic phase identification enabled the establishment of a degradation mechanism initiated by external silica contamination, followed by lubricant film breakdown, abrasive wear, adhesive wear, tribocorrosion, and ultimately functional blockage of the bearing. This integrated multiscale approach provided a comprehensive understanding of the degradation process and supported the identification of the root cause of failure under actual industrial operating conditions.

3. RESULTS

3.1 Macroscopic evidence of the failure

Initial inspection of the NU240 bearing, carried out after progressive braking was detected throughout its rotation, revealed lubricant of abnormally high density and brown corrosion products deposited on the outer and intermediate surfaces of the component. After cleaning the parts following the procedure of ASTM G1-03(2017)e1 described in Section 2.3 [11] (Figure 1), the bearing showed severe deterioration of the contact surfaces, together with a substantial loss of the rolling elements' rotational capability. The inner and outer raceways exhibited dark-colored regions, adhered deposits, and areas of localized wear, while the cylindrical rollers showed surface deformation and accumulation of solid particles.

Fig. 1. NU240 bearing after cleaning following the ASTM procedure.

These observations indicate that the system underwent progressive degradation during operation, ruling out an instantaneous failure event and suggesting a cumulative mechanism associated with unfavorable tribological conditions. Fractographic analysis of one region of the bearing (Figure 2) further revealed anomalous plastic deformation for this type of component, possibly related to the assembly of the unit on the pelletizer shaft [12].

(a) (b)

Fig. 2. Regions of the bearing showing anomalous plastic deformation, possibly associated with assembly of the unit.

During disassembly, a considerable amount of solid debris mixed with the lubricant was identified, together with compacted deposits on the cage and raceways. Once the steel raceways and cylindrical rollers were separated (Figure 3), highly deteriorated zones were observed with galvanic-type corrosion products, generated by the ionic exchange characteristic of prolonged immersion in the lubricant between anodic and cathodic regions of the metal surface [13].

(a)

(b)

Fig. 3. (a) General view of the bearing's metal raceway, showing galvanic corrosion and surface deterioration, (b) Detail of the metal raceway showing anodic and cathodic zones associated with galvanic corrosion.

The simultaneous presence of metallic material and mineral particles in the collected solid debris suggests progressive degradation of the lubricant film, which allowed direct contact between the surfaces and favored the continuous generation of wear particles. These macroscopic alterations are consistent with patterns described for failures induced by solid contamination in rolling-element bearings, in which the loss of effective lubrication accelerates the transition from a moderate wear regime to combined mechanisms of abrasion, adhesion, and corrosion [14].

3.2 Morphological characterization of the wear mechanisms

Optical microscopy identified different deterioration mechanisms distributed over the raceways and rolling elements. In the region shown in Figure 4, abrasive wear is observed on the steel raceway, with particle accumulation and appreciable material removal in the outer grooved areas, as well as particle embedding in the central region. This pattern is consistent with the ingress of external contaminant particles into the lubrication system. At the edges of the same region, particles detached from the bearing itself are observed, attributable to cavitation, most likely caused by the absence of an adequate filtration system in the lubrication circuit.

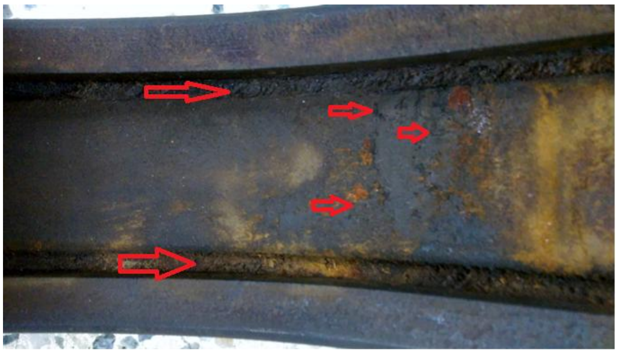

Fig. 4. Raceway region showing abrasive wear, particle accumulation, and material detachment.

In an adjacent region of the raceway (Figure 5), cavitation wear was identified, characterized by material detachment associated with the intermittent implosion of bubbles generated by abrupt pressure changes in the oil, preferentially located along the direction of maximum applied load. Metallographic magnification of this area (Figure 6) revealed regions of extensive surface destruction, with cavity formation attributable to excessive vibration, oil contamination with abrasive particles capable of promoting foam formation, and inadequate clearance between the shaft and the bearing [15]; the striations observed in the central part of these images correspond to superimposed abrasive wear.

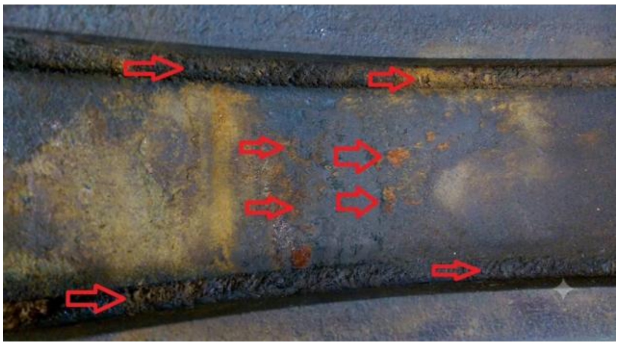

Fig. 5. Raceway region showing cavitation wear in the direction of maximum load.

(a) (b)

Fig. 6. Metallographic detail (40×) of the cavitation zones, with superimposed abrasive-wear striations.

In another region of the steel raceway (Figure 7), adhesive wear was identified, generated by direct contact between the bearing and the roller following total loss of the lubricant film. This mechanism can be associated with cold starts with low oil flow due to high viscosity, obstructions or leaks in the lubrication circuit, or misalignments that promote rubbing between the shaft and the bearing.

Fig. 7. Adhesive wear present on the steel raceway, resulting from direct contact between metal surfaces.

Fractographic analysis of the cylindrical rollers removed from the bearing (Figure 8) showed a deterioration pattern similar to that identified on the contacting steel raceways, dominated by abrasive wear. The corresponding micrographs (Figure 9) confirmed extensive areas where abrasive wear removed a considerable fraction of the metal surface; at 40× (Figure 9a), adhered metallic material is observed on the surface, while at 68× (Figure 9b), bronze-type material transferred from the cage to the roller is identified, evidencing that abrasive wear simultaneously affected the three components making up the bearing [16].

(a) (b)

Fig. 8. Cylindrical rollers removed from the bearing, showing deterioration consistent with that observed on the steel raceways.

Finally, analysis of the bronze cage (Figure 10) revealed advanced adhesive wear, with transfer of metallic material from the steel roller, a direct consequence of insufficient lubrication between the parts [17]. Micrographs of two different regions of the cage (Figure 11) confirm zones of severe adhesive wear and appreciable metallic mass loss, evidencing that the degradation phenomenon affected the three main bearing components in a generalized manner.

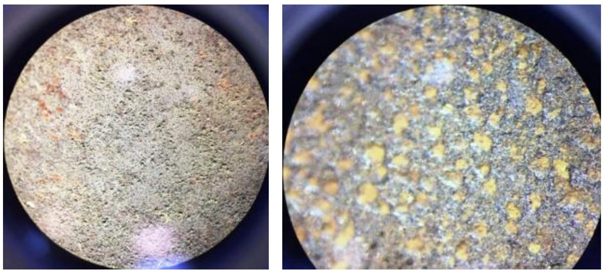

(a) (b)

Fig. 9. Micrographs of the roller surface: (a) 40×, adhered metallic material; (b) 68×, transfer of bronze-type material onto the roller.

Fig. 10. Wear present on the bronze cage, resulting from contact between metal parts and deficient lubrication.

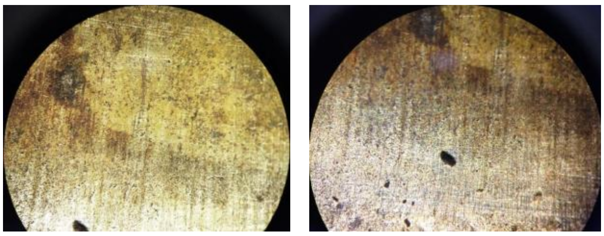

(a) (b)

Fig. 11. Cage regions in direct contact with the rollers, showing accelerated wear due to part deformation.

3.3 Physicochemical characterization of the lubricant by FTIR

The FTIR spectra obtained for the lubricant samples (Figures 12 and 13) showed, in addition to the characteristic bands of the organic oil matrix, signals corresponding to inorganic substances foreign to the original composition of the lubricant [18]. It should be noted that FTIR is primarily a qualitative technique: it does not allow direct quantification of the concentration of the identified contaminant, since the obtained signal depends on multiple factors, including particle size, distribution within the matrix, and spectral overlap with the organic bands of the oil; nonetheless, it enables the unambiguous molecular identification of the species present through their characteristic vibrational bands. In both spectra, the signals matched the SiO_2 reference patterns closely and consistently between the two samples analyzed, confirming the ingress of silica particles (sand or quartz) into the lubrication system.

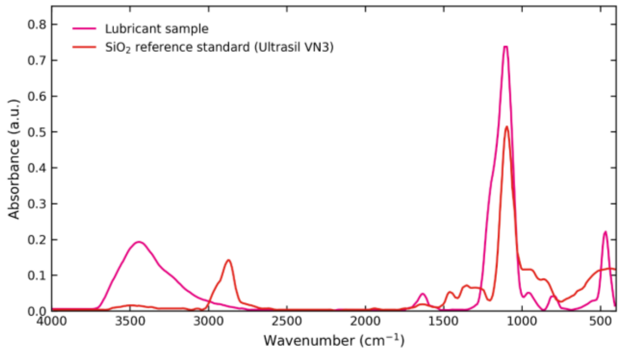

Fig. 12. FTIR spectrum of oil sample 1, showing the presence of SiO_2 particles.

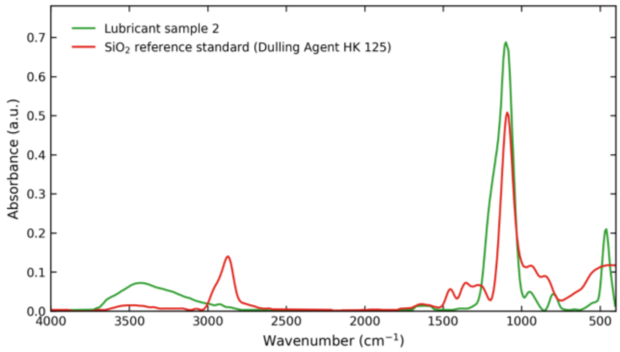

Fig. 13. FTIR spectrum of oil sample 2, confirming the presence of SiO_2 together with the other lubricant constituents.

Owing to their high hardness and angular morphology, these ceramic particles promote micro-cutting processes and abrasive wear, progressively increasing the surface roughness of the raceways. The FTIR results thus constitute a first, chemical line of evidence of external contamination of the lubrication system, consistent with the morphological evidence described in Section 3.2.

3.4 Identification of corrosion products and contaminants by XRD

The diffractogram obtained for the metal surface of the radial bearing (Figure 14) identified magnetite and goethite as the main corrosion products, together accounting for 88.2%, along with a SiO_2 fraction close to 12%. This result is consistent with the severe wear observed on the metal parts and confirms the simultaneous presence of oxidation phenomena and mineral contamination.

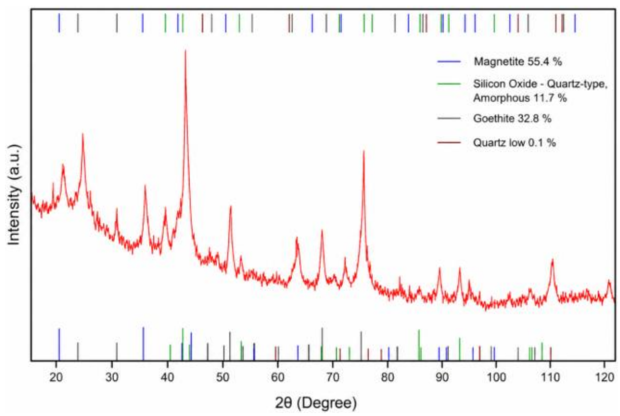

Fig. 14. Diffractogram of the metal surface of the NU240 radial bearing.

Analysis of the solid debris collected between the bearing parts (Figure 15), with an appearance corresponding to solidified lubricant, likewise showed corrosion products (magnetite and goethite) totaling 82%, together with 18% SiO_2 [19]. Based on this evidence, it was established that the contaminant responsible for the wear of the parts is of external origin, resides within the lubricant, and, due to the continuous movement of the components, tends to deposit on previously worn metal areas.

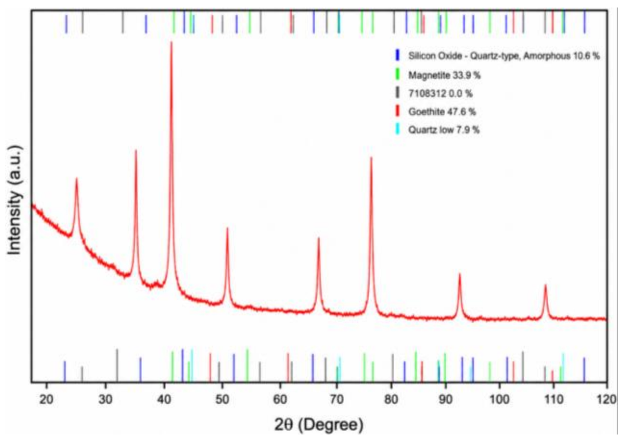

Fig. 15. Diffractogram of the solid debris recovered from the lubricant, showing corrosion products and SiO_2.

As a complementary sample, the roller surface of the 89456M axial bearing (Figure 16), which had been exposed to the environment, was also analyzed. In this case, magnetite was identified as the sole corrosion product, at a high proportion (71%) associated with sediments formed in an aqueous medium [20], together with a SiO_2 fraction of 29%. This result confirms that both the parts removed from the axial bearing and those from the radial bearing show an appreciable content of contaminant particles, and suggests that the higher relative proportion of silica in the axial roller may be related to its greater density relative to the lubricant, which favors its progressive sedimentation compared with particles suspended in the circulating oil.

Table 1 summarizes the phase composition identified by XRD at the three sampling points analyzed, evidencing a consistent pattern of silica contamination throughout the tribological system.

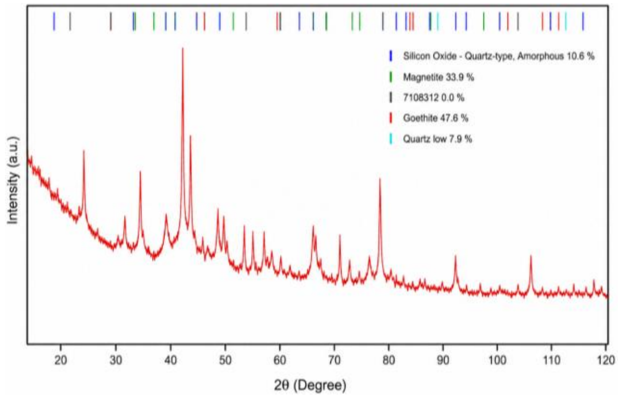

Fig. 16. Composition spectrum of the contaminants identified on the roller of the 89456M axial bearing.

It should be noted that the phase percentages reported in Table 1 correspond to semi-quantitative estimations obtained with the X'Pert HighScore software described in Section 2.5, and should therefore be interpreted as indicative of the relative proportion between corrosion products and SiO_2 rather than as absolute quantitative values.

Table 1. Phase composition identified by XRD at the different sampling points.

Sampling point	Iron oxides (magnetite + goethite) [%]	SiO_2 [%]
Metal surface of the NU240 radial bearing (Fig. 14)	88.2	12.0
Solid debris from the lubricant, radial bearing (Fig. 15)	82.0	18.0
Roller surface, 89456M axial bearing (Fig. 16)	71.0	29.0

3.5 Integration of the failure mechanism

The integration of the evidence obtained from visual inspection, microscopy, FTIR, and XRD allowed a progressive bearing-degradation mechanism to be established, summarized schematically in Figure 17. Initially, the ingress of silica particles contaminated the lubricant and altered the tribological conditions of the contact; these particles acted as an abrasive third body, generating micro-cutting on the raceways and promoting increased surface roughness.

As abrasive wear progressed, the lubricant film lost continuity, allowing direct contact between the metal surfaces and promoting adhesive wear mechanisms. The continuous generation of metallic particles further increased lubricant contamination, while the rise in temperature and exposure of the base material favored the formation of magnetite and goethite as corrosion products. Finally, the combined action of abrasion, adhesion, and tribocorrosion produced a progressive increase in the resistance to motion of the rolling elements, culminating in functional blockage of the bearing and loss of system operability.

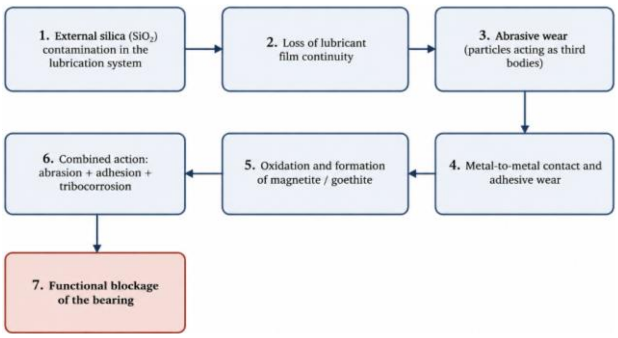

Fig. 17. Schematic of the proposed failure mechanism for the NU240 bearing, from external silica contamination to functional blockage of the component.

4. DISCUSSION

The evidence obtained in this work, derived from a real case of industrial operation, is consistent with findings reported in controlled laboratory tests on grease and oil contamination with SiO_2 particles. Ta et al. [7] demonstrated that the presence of environmental particles and water in lubricating greases measurably increases friction, wear, and pitting formation, while Ikhsan et al. [6] reported wear patterns directly attributable to the concentration and size of solid contaminant particles in ball bearings. The present analysis extends these laboratory observations to an in-service failure case, showing that the same causal chain (silica contamination, lubricant film loss, abrasion, adhesion, and corrosion) can be reconstructed from morphological and physicochemical evidence in a real industrial component, reinforcing the diagnostic value of the methodology employed.

The failure sequence identified here is also consistent with previously reported industrial and field investigations of rolling-element bearings. Gurumoorthy and Ghosh [12] similarly traced the failure of a taper roller bearing to the combined action of contamination and inadequate lubrication, while Maru et al. [14] showed, through vibration and wear analysis, that solid contamination progressively degrades bearing performance even when it is not immediately detected by routine monitoring. Morales-Espejel and Zhou [8] further emphasized that visual and morphological inspection remains an effective diagnostic route for particle-contamination damage, in agreement with the multiscale approach adopted in the present work. Taken together, these studies support the generality of the degradation sequence (contamination, lubricant film breakdown, abrasion, adhesion, and corrosion) identified in the NU240 bearing, and reinforce the relevance of the proposed methodology beyond this single case.

A particularly relevant finding for maintenance practice is the discrepancy observed between routine lubricant monitoring reports, which indicated wear-metal and silicon concentrations within the manufacturer's established limits, and the actual evolution of the failure, which culminated in functional blockage of the bearing. This discrepancy suggests that the alert thresholds used in conventional oil-analysis programs may not be sufficiently sensitive to detect progressive ceramic-particle contamination at early stages, particularly in systems with low sampling frequency or inadequate filtration [21]. Consequently, it is recommended that routine monitoring be complemented with techniques of greater structural specificity, such as FTIR or XRD, when operational symptoms of deterioration are not explained by conventional reports.

From a normative classification standpoint, the mechanisms identified (abrasion, adhesion, cavitation, and corrosion) correspond to recognized damage categories in ISO 15243:2017 [9] and the SKF Bearing Damage Atlas [10], allowing the findings of this case to be situated within a reference framework widely accepted in industry and facilitating their transfer to other predictive-maintenance contexts.

This work presents limitations inherent to a field failure analysis: because it involves a single case of industrial operation, it was not possible to isolate variables such as the exact particle concentration, the contaminant ingress rate, or the temporal evolution of the friction coefficient, as can be done in laboratory tests under controlled conditions. As future work, it is recommended that this type of analysis be complemented with controlled tribological tests, following protocols similar to those of Ta et al. [7] and Ikhsan et al. [6], to quantify the wear rate as a function of silica concentration, as well as incorporating scanning electron microscopy (SEM) and energy-dispersive spectroscopy (EDS) for a more detailed characterization of the morphology and elemental composition of the wear particles.

5. CONCLUSION

The comprehensive analysis of the NU240 radial bearing removed from an industrial pelletizer established that the root cause of its failure was external contamination of the lubrication system by silica (SiO_2) particles, consistently identified by FTIR in the lubricant and by XRD on the bearing's metal surface, in the recovered solid debris, and in a complementary axial bearing.

The morphological and structural evidence allowed a progressive degradation sequence to be reconstructed: the ingress of silica particles generated third-body abrasive wear, which progressively reduced the continuity of the lubricant film and promoted metal-to-metal contact and the development of adhesive wear; the combination of both mechanisms, together with the formation of magnetite and goethite as corrosion products, ultimately led to functional blockage of the bearing.

The absence of an effective filtration system in the lubrication circuit was identified as the operational factor that allowed the ingress and persistence of contaminant particles in the system, while the persistence of deterioration symptoms despite routine lubricant readings within the manufacturer's limits highlights the need to review the sensitivity of the monitoring criteria used in predictive maintenance programs.

The integrated methodology of visual inspection, fractography, optical microscopy, FTIR, and XRD proved effective in establishing the root cause of the failure and is replicable for diagnosing other lubricated transmission systems subjected to severe industrial conditions. It is recommended to incorporate higher-efficiency filtration systems, adjust the frequency and sensitivity of lubricant-contamination monitoring, and validate, through controlled laboratory tests, the quantitative relationship between silica concentration and wear rate, in order to strengthen predictive-maintenance strategies and extend the service life of industrial bearings.

Acknowledgement

The authors gratefully acknowledge the Universidad Militar Nueva Granada, Bogotá, Colombia, for the institutional and financial support provided to the Department of Engineering, which made this research possible.

REFERENCES

[1] H. Peng, H. Zhang, L. Shangguan, and Y. Fan, "Review of tribological failure analysis and lubrication technology Research of wind power bearings," *Polymers*, vol. 14, no. 15, p. 3041, Jul. 2022, doi: 10.3390/polym14153041.

[2] G. W. Stachowiak and A. W. Batchelor, *Engineering tribology*, 4th edition. Oxford: Elsevier/Butterworth-Heinemann, 2014.

[3] Y. N. Aldeoes, P. Gokhale, and S. Y. Sondkar, "A review of predictive maintenance of bearing failures in rotary machines by predictive Analytics using Machine-Learning techniques," in *Signals and communication technology*, 2023, pp. 115–138. doi: 10.1007/978-3-031-29713-7_6.

[4] T. A. Harris and M. N. Kotzalas, *Advanced concepts of bearing technology: Rolling Bearing Analysis, Fifth Edition*. CRC Press, 2006.

[5] [R. De La Presilla, S. Wandel, M. Stammler, M. Grebe, G. Poll, and S. Glavatskih, "Oscillating rolling element bearings: A review of tribotesting and analysis approaches," *Tribology International*, vol. 188, p. 108805, Jul. 2023, doi: 10.1016/j.triboint.2023.108805.

[6] A. Ikhsan, D. Gasni, and M. Rusli, "Wear Patterns on Ball Bearings Lubricated by Grease Contaminated with Several Large Solid Particles," *Tribology in Industry*, vol. 47, no. 2, pp. 202–2016, Jun. 2025, doi: 10.24874/ti.1893.02.25.04.

[7] T.-N. Ta, J.-H. Horng, M.-W. Huang, E. V. Torskaya, and C.-W. Kuo, "Tribological characteristics and vibration response of grease lubricated contacts under environmental particles and water impact," *Wear*, vol. 550–551, p. 205403, May 2024, doi: 10.1016/j.wear.2024.205403.

[8] G. E. Morales-Espejel and Y. Zhou, "Rolling Bearing Damage from Particle Contamination – Diagnosis via Inspection," *Tribology Online*, vol. 19, no. 1, pp. 95–104, Mar. 2024, doi: 10.2474/trol.19.95.

[9] International Organization for Standardization, *Rolling Bearings—Damage and Failures—Terms, Characteristics and Causes*, ISO 15243:2017, Geneva, Switzerland, 2017.

[10] SKF Group, *Bearing Damage and Failure Analysis*. Gothenburg, Sweden: SKF Group, 2014.

[11] ASTM International, *Standard Practice for Preparing, Cleaning, and Evaluating Corrosion Test Specimens*, ASTM G1-03(2017)e1, West Conshohocken, PA, USA, 2017, doi: 10.1520/G0001-03R17E01.

[12] K. Gurumoorthy and A. Ghosh, "Failure investigation of a taper roller bearing: A case study," *Case Studies in Engineering Failure Analysis*, vol. 1, no. 2, pp. 110–114, Apr. 2013, doi: 10.1016/j.csefa.2013.05.002.

[13] M. Kronberger and J. Brenner, "Tribocorrosive Aspects of Tungsten Carbide, Silicon Nitride, and Martensitic Steel under Fretting-like Conditions," *Lubricants*, vol. 11, no. 5, p. 195, Apr. 2023, doi: 10.3390/lubricants11050195.

[14] M. M. Maru, R. S. Castillo, and L. R. Padovese, “Study of solid contamination in ball bearings through vibration and wear analyses,” *Tribology International*, vol. 40, no. 3, pp. 433–440, Jun. 2006, doi: 10.1016/j.triboint.2006.04.007.

[15] A. Qi, M. Priest, C. M. Taylor, R. M. Mortier, D. D. Parker, and W. H. Preston, “Experimental study of the influence of bubbly oil on cavitation erosion of engine journal bearing materials,” in *Tribology series*, 2001, pp. 111–119. doi: 10.1016/s0167-8922(01)80098-5.

[16] S. Laumann, R. Jisa, G. Deinhofer, and F. Franek, “Tribological properties of brass materials and their application for cages in rolling bearings,” *Tribology - Materials Surfaces & Interfaces*, vol. 8, no. 1, pp. 35–40, Nov. 2013, doi: 10.1179/1751584x13y.0000000052.

[17] R. Demirsöz, “Wear Behavior of Bronze vs. 100Cr6 Friction Pairs under Different Lubrication Conditions for Bearing Applications,” *Lubricants*, vol. 10, no. 9, p. 212, Sep. 2022, doi: 10.3390/lubricants10090212.

[18] F. R. Van De Voort, J. Sedman, R. A. Cocciardi, and D. Pinchuk, “FTIR Condition Monitoring of In-Service lubricants: ongoing developments and future perspectives,” *Tribology Transactions*, vol. 49, no. 3, pp. 410–418, Jul. 2006, doi: 10.1080/10402000600781432.

[19] R. A. Antunes, R. U. Ichikawa, L. G. Martinez, and I. Costa, “Characterization of corrosion products on carbon steel exposed to natural weathering and to accelerated corrosion tests,” *International Journal of Corrosion*, vol. 2014, pp. 1–9, Jan. 2014, doi: 10.1155/2014/419570.

[20] H. Tanaka, R. Mishima, N. Hatanaka, T. Ishikawa, and T. Nakayama, “Formation of magnetite rust particles by reacting iron powder with artificial α-, β- and γ-FeOOH in aqueous media,” *Corrosion Science*, vol. 78, pp. 384–387, Sep. 2013, doi: 10.1016/j.corsci.2013.08.023.

[21] ASTM International, *Standard Guide for Statistically Evaluating Measurand Alarm Limits When Using Oil Analysis to Monitor Equipment and Oil for Fitness and Contamination*, ASTM D7720-21, West Conshohocken, PA, USA, 2021, doi: 10.1520/D7720-21.